

## ANTIQUÉ WOOD PREPARATION BY INORGANIC SALTS

### TREATMENT AND ITS PERFORMANCE

Ming Sun<sup>1</sup> <https://orcid.org/0000-0001-5286-9355>

Chencheng Zhao<sup>1</sup> <https://orcid.org/0000-0001-6607-8714>

Courage Alorbu<sup>2</sup> <https://orcid.org/0000-0001-5193-4290>

Youming Yu<sup>1\*</sup> <https://orcid.org/0000-0002-2184-8890>

Lili Cai<sup>2\*</sup> <https://orcid.org/0000-0002-2099-4837>

<sup>1</sup> Zhejiang A&F University, College of Chemistry and Materials Engineering, Hangzhou, China.

<sup>2</sup> University of Idaho, Department of Forest, Rangeland and Fire Sciences, Moscow, Idaho.

\*Corresponding author: [yuyouming@zafu.edu.cn](mailto:yuyouming@zafu.edu.cn), [lcai@uidaho.edu](mailto:lcai@uidaho.edu)

**Received:** December 15, 2021

**Accepted:** March 02, 2023

**Posted online:** March 03, 2023

#### ABSTRACT

Conservation of historic timber structures is of great importance for cultural inheritance and community identity promotion. However, most of the current methods available for ancient architecture protection significantly affect their original appearance and aesthetic value and finding wood elements that are similar to the ones in existing historic timber structures is not easy. Here we report a simple and effective method to archaize wood, *Castanopsis sclerophylla*, by ferric chloride (FeCl<sub>3</sub>) treatment without significantly affecting its mechanical properties and durability. The lightness and the color indexes of treated wood are similar to the ancient wood sample. The mechanical properties of FeCl<sub>3</sub> treated wood are not statistically different from the control. Our durability testing results indicated that FeCl<sub>3</sub> treated wood has good decay resistance against *Irpex lacteus* and *Trametes versicolor* with a mass loss of less than 10 %. This study provides a convenient method for the restoration and protection of ancient buildings.

**Keywords:** Ancient wood, fungal resistance, historic timber structures, inorganic salt, mechanical properties.

33

## 34 INTRODUCTION

35 As history and culture carriers, ancient Chinese architecture is a combination of feng shui,  
36 philosophy, art and technology, which is of great significance to cultural inheritance and is  
37 worth being protected in many aspects (Yin 2019). These ancient Chinese architecture buildings  
38 are mainly in wooden structures, including temples (Li and Zhang 2007), courtyards (Li and  
39 Lian 2021), wooden pagodas (Du *et al.* 2002), palaces (Sun 2010), etc. However, due to the  
40 anisotropic feature of wood, intrinsic susceptibility of wood to deterioration and vandalism of  
41 the historical architectures, the present situation of ancient wooden buildings protection is not  
42 optimistic (Yang *et al.* 2020, Zhang *et al.* 2013).

43 The common damage of these historic timber structures includes structural deformation,  
44 cracking and decay (Shi and Yong 2014). To solve these problems, there are several established  
45 methods to repair or reinforce ancient wooden structures, depending on the degree of damage.  
46 The minor damaged part of the wooden building is typically filled with wood flour, unsaturated  
47 polyester resins, fiber-reinforced polymers (Zhao *et al.* 2019), carbon nanotubes (Marzi 2015)  
48 or other chemical materials (Cao *et al.* 2015) while in more severe cases, the damaged wood  
49 structures are usually reinforced with metal-based materials or tensile bars. In terms of  
50 completely decayed wooden components, new wood parts or other materials (Chun *et al.* 2013,  
51 Que *et al.* 2017) will be used. For example, Yan *et al.* (2012) found that the seismic behavior  
52 of the timber-framed structure can be reinforced with iron hooks. Triantafillou and Deskovic  
53 (1992) reported that wooden beams that were externally bonded with fiber-reinforced plastic  
54 sheets using epoxy adhesives have strengthened performance. Zhou *et al.* (2020)'s research  
55 revealed that ethyl orthosilicate and methyl triethoxysilane improved the performance of  
56 decayed wood. Although these approaches preserve the structural integrity of the wooden  
57 structures, they all greatly affect the aesthetic appearance of ancient buildings. Using wood  
58 elements that have a similar color to the ancient wooden building is the most simple and  
59 sustainable way to repair and restore damaged wooden structures while allowing for their  
60 enhanced cultural and aesthetic values.

61 Since most methods available for historic timber structures protection significantly affect  
62 their original appearance and aesthetic value, and finding wood elements that are similar to the  
63 ones in existing historic timber structures is not easy, we propose a method of archaizing wood  
64 without damaging the mechanical properties and durability of wood. This idea is based on  
65 previous reports by manipulating inorganic salt treatment on wood, the color of treated wood  
66 could be as close to the one in the existing wooden building while not significantly affecting  
67 the overall performance of wood (Dong 2016, Wang 2017). For example, it was found that the  
68 surface color of Chinese fir and larch is closely related to the treating concentration of sodium  
69 hydroxide (Dong 2016) and by using different inorganic salts, and treating procedures, the color  
70 of wood can reach the target color while not significantly affecting the mechanical properties  
71 of wood (Wang 2017). However, the use of multistep inorganic salt treatments, including  
72 sodium hydroxide (NaOH), sodium sulfite (Na<sub>2</sub>SO<sub>3</sub>) and FeCl<sub>3</sub>, for wood coloration and how  
73 these treatments affect the mechanical properties and durability of wood have not been reported  
74 (Chen *et al.* 2005).

75 *Castanopsis sclerophylla* is very common evergreen broad-leaved tree species in South  
76 China which also exhibit good comprehensive performance. (Ding *et al.* 2020) It has been  
77 widely used as the material for buildings, bridges and furniture more than 700 years in China.  
78 Therefore, in this paper, *Castanopsis sclerophylla* was chosen as the raw material to investigate  
79 antique mechanism for the repairment of ancient buildings. The objectives of this study are to  
80 investigate the effect of the above-mentioned inorganic salt treatments on the chemical structure  
81 of hardwood, *Castanopsis sclerophylla*, which was frequently used as pillars and purlins of  
82 beams (Yang 2019) in historic wooden structures. The changes in color, mechanical properties  
83 and durability against white-rot wood decay fungi were also reported.

84

## 85 **MATERIALS AND METHODS**

### 86 **Materials**

87 Sapwood specimens of *Castanopsis sclerophylla* with no visible defects were cut into  
88 various sizes. The size of the samples for flexural test, compressive strength parallel to grain

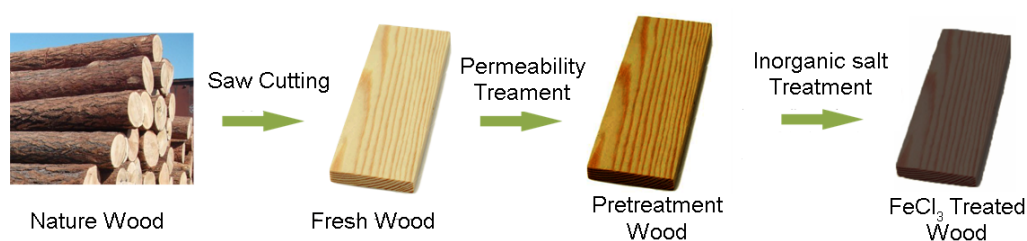
89 test and soil block test was 10 mm × 10 mm × 150 mm ( $R \times T \times L$ ), 10 mm × 10 mm × 15 mm  
90 ( $R \times T \times L$ ) and 14 mm × 14 mm × 14 mm ( $R \times T \times L$ ), respectively. These samples were  
91 conditioned at room temperature with a relative humidity of 50 % to constant weight before  
92 further analysis.

93 Sodium hydroxide (NaOH), sodium sulfite ( $\text{Na}_2\text{SO}_3$ ), ferric chloride ( $\text{FeCl}_3$ ) and  
94 hydrochloric acid (HCl) were purchased from Shanghai Aladdin Bio-Chem Technology Co.,  
95 LTD for inorganic salt treatment. All these chemicals were of chemical grade. Two white-rot  
96 fungi, *Irpex lacteus* (*I.l.*) and *Trametes versicolor* (*T.v.*) were obtained from ATCC (Manassas,  
97 VA).

98

### 99 $\text{FeCl}_3$ treatment on wood

100 The inorganic salt treatment of wood includes two steps, as shown in Figure 1. Briefly,  
101 before  $\text{FeCl}_3$  solution treatment and to increase the permeability of the wood, the wood samples  
102 were soaked in a mixed solution of 2 M NaOH and 0,5 M  $\text{Na}_2\text{SO}_3$  at 60 °C for 2 min.  
103 Subsequently, the pretreated wood samples were immersed in 0,1 M HCl for 1 min to neutralize  
104 the residual alkaline solution on the surface of wood and were further soaked in 0,1 M  $\text{FeCl}_3$   
105 solution for 5 min to 10 min at room temperature, depending on the sample sizes. The samples  
106 were left at room conditions until constant mass.



107 **Figure 1:** The flow diagram for  $\text{FeCl}_3$  treatment on wood.

108

### 109 FTIR Analysis

110 Fourier transform infrared spectrometer (NICOLET IMPACT410, NICOLET, Madison,  
111 Wisconsin, USA) was used to identify the functional groups of the components. Both the  
112 untreated and  $\text{FeCl}_3$  treated samples were mixed with potassium bromide (KBr) at a weight

113 ratio of 1:100 and pressurized using a tableting method. The IR spectra were recorded with a  
114 scanning wavenumber range of  $400\text{ cm}^{-1}$  -  $4000\text{ cm}^{-1}$  and a scanning resolution of 32. The  
115 treated samples were collected from 1 mm below the surfaces of wood along the growth  
116 direction and were grounded into 200 mesh before mixing with KBr. The spectra were baseline-  
117 corrected and normalized before analysis.

118

### 119 **Static Bending Test and Compression Parallel to Grain**

120 Flexural properties of the  $\text{FeCl}_3$  treated wood samples were determined through a three-  
121 point static bending test using an Instron (Instron 5967, Norwood, MA). A load of 30 kN was  
122 applied at a crosshead speed of 5 mm/min to obtain a load-deflection curve. The maximum load  
123 at the proportional limit of the curve and the failure curve were used to calculate the modulus  
124 of rupture (MOR) and modulus of elasticity (MOE) GB/T 1936.1-2009; GB/T 1936.2-2009  
125 (SAC 2009a; SAC 2009b), respectively. The corresponding equations were listed below (Eq.1-  
126 2):

$$127 \text{ Modulus of Rupture (MOR)} = \frac{3F_{\max}l}{2bt^2} \quad (1)$$

128

$$129 \text{ Modulus of Elasticity (MOE)} = \frac{l^3}{4bt^3} \times \frac{\Delta F}{\Delta f} \quad (2)$$

130 Where  $b$  and  $t$  are the width and thickness of the specimen, respectively;  $l$  is the span of  
131 support, which is 120 mm;  $F_{\max}$ ,  $\Delta F$  and  $\Delta f$  are load at failure, load increment and deflection  
132 increment, respectively.

133 For compressive strength parallel to the grain test, the wood samples were placed in the  
134 center of the spherical moving support of the testing machine and a load of 30 kN at a crosshead  
135 rate of 1 mm/min was applied to the samples. The compressive strength of the samples was  
136 calculated per the following equation (Eq. 3) GB/T 1935-2009 (SAC 2009c):

$$137 \text{ Compressive Strength Paralle to Grain of Wood } (\sigma) = \frac{P_{\max}}{bt} \quad (3)$$

138 Where  $\sigma$ ,  $P_{\max}$ ,  $b$  and  $t$  are strength parallel to the grain of wood, load at failure, width and  
139 thickness of the specimen, respectively.

140

### Color Change after Inorganic Salt Treatment

Color evaluation of the wood samples before and after treatment was determined in the CIE  $L^*a^*b^*$  color space by a colorimeter (DC-P3) (Janin 1994).  $L^*$  means the lightness from black (0) to white (100) while  $a^*$  and  $b^*$  represent chromaticity indices where  $+a^*$  is red,  $-a^*$  is green,  $+b^*$  is yellow and  $-b^*$  is blue. The total color difference ( $\Delta E^*$ ) was defined according to the equation given below (Eq. 4):

$$\Delta E^* = \sqrt{(\Delta L^*)^2 + (\Delta a^*)^2 + (\Delta b^*)^2} \quad (4)$$

where  $\Delta L^*$ ,  $\Delta a^*$ ,  $\Delta b^*$  are the difference of  $L^*$ ,  $a^*$  and  $b^*$  before and after treatment, respectively. All the color measurements were taken in the longitudinal directions with 3 replicates (3 measuring points along the diagonal line for each treatment) and the average value was reported.

### Leaching test for $\text{FeCl}_3$ treated wood

The leaching of wood samples in water was conducted according to the AWWA E11-16 (AWWA 2016a) with a minor modification on the amount of water used. Briefly, 12 replicate samples of untreated and  $\text{FeCl}_3$  treated wood cubes were fully submerged and weighed down in 78 mL DI water in a beaker to prevent floating. After 1 hour of immersion, the first leachate was collected and replaced with fresh DI water. The beakers were then placed on an orbital shaker and agitated at 100 rad/min for 6 hours, after which the leachate was again collected and replaced with 78 mL fresh DI water. The procedure was repeated for 24 h, 48 h, and thereafter at 48 h intervals, for a total period of 14 days to collect 9 leachates. The leaching test was conducted at room conditions. After the last leachate was collected, the wet mass of the samples and thereafter the final oven-dried mass of the wood cubes were reordered.

### Fungal decay resistance test

Fungal resistance of untreated and  $\text{FeCl}_3$  treated wood samples was conducted according to AWWA E10-16 (AWWA 2016b) with two modifications. First, malt-agar substrate, instead of soil, was used for the durability test. Another modification was that both unleached and leached specimens were sterilized by spraying 70 % ethanol on the surface of the samples in the

170 laminated hood for 2 h. Both untreated (control) and FeCl<sub>3</sub> treated specimens with and without  
171 leaching were inoculated onto the top of feeder strips that were covered by actively growing  
172 fungus, either *I.l.* and *T.v.* The culture bottles were then incubated in an environmental chamber  
173 at 75 % humidity and 25 °C in the dark for eight weeks. At the end of the exposure period, the  
174 wet mass and the oven-dried mass of the exposed cubes were recorded. The mass loss was  
175 calculated according to the following equation (Eq. 5):

$$176 \quad \text{Mass Loss \%} = \frac{(m_{\text{unexpo.}} - m_{\text{expo.}})}{m_{\text{unexpo.}}} \times 100 \% \quad (5)$$

177 Where  $m_{\text{unexpo.}}$  and  $m_{\text{expo.}}$  are the oven-dried mass of untreated or treated sample before and  
178 after exposure to fungi respectively.

179

### 180 **Statistical Analysis**

181 The mechanical properties data and durability results were statistically analyzed using  
182 Statistical Analysis System software (SAS version 9.4, SAS Institute, Cary, NC). The data were  
183 compared using a one-way analysis of variance (ANOVA) at the 95 % confidence level (Littell  
184 1998).

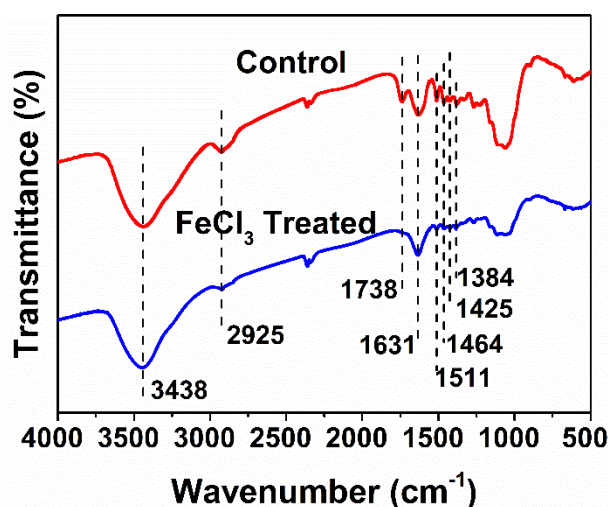
185

## 186 **RESULTS AND DISCUSSION**

### 187 **FTIR analysis**

188 Figure 2 shows the FTIR spectra of control and FeCl<sub>3</sub> treated samples. In control, the peak  
189 at 3438 cm<sup>-1</sup> is attributed to wood-specific O-H stretching vibration. The peak at 2925 cm<sup>-1</sup> is  
190 due to stretching vibrations of methyl, methylene, or methylene (Zhang *et al.* 2019). The  
191 absorption band at 1738 cm<sup>-1</sup> corresponds to the acetyl group in hemicellulose. The absorption  
192 band at 1631 cm<sup>-1</sup> is related to the stretching vibration of C=O. The peaks at 1511 cm<sup>-1</sup> and  
193 1464 cm<sup>-1</sup> correspond to the stretching vibration of the benzene ring caused by the vibration of  
194 the lignin aromatic skeleton. Absorption peaks at 1425 cm<sup>-1</sup> and 1384 cm<sup>-1</sup> correspond to the  
195 C-H deformation in lignin and carbohydrates. After inorganic salt treatment, the peak at 1738  
196 cm<sup>-1</sup> in the spectrum of the treated sample disappeared, indicating the loss of hemicellulose  
197 due to the treatment effect. Moreover, the intensities of the peaks from 1400 cm<sup>-1</sup> to 1600 cm<sup>-1</sup>

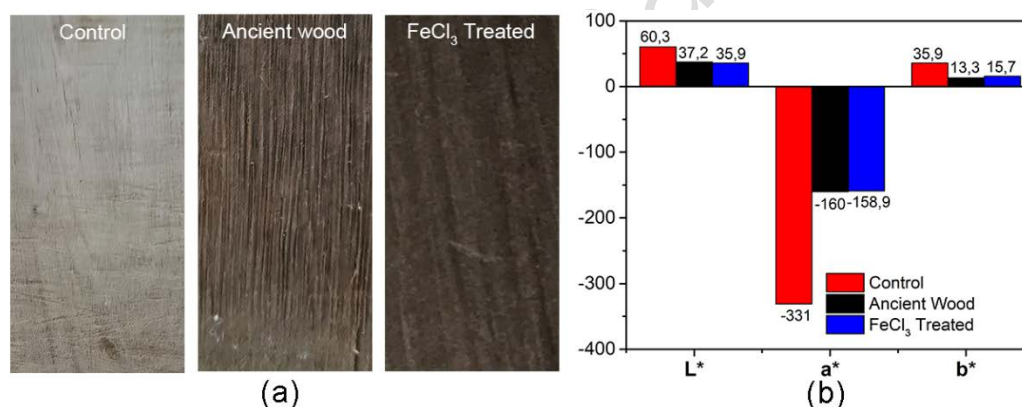
198 <sup>1</sup> were weakened, possibly related to the partial removal of lignin in FeCl<sub>3</sub> treated wood (Zhang  
 199 *et al.* 2019).



200  
 201 **Figure 2:** Fourier-transform infrared spectra (FTIR) of untreated and FeCl<sub>3</sub> treated samples.

202

203 **Color measurement**



204 **Figure 3:** a) Photos of wood samples before and after treatment, b) Surface color parameters  
 205 of control, ancient wood and FeCl<sub>3</sub> treated wood samples.

206

207 **Table 1:** The color difference ( $\Delta E^*$ ) of control, ancient wood and FeCl<sub>3</sub> treated wood  
 208 samples.

$\Delta E^*$	Control Sample	Ancient wood Sample	Treated Sample
Control Sample	0	172,8	173,9
Ancient Wood Sample	172,8	0	2,9
Treated Sample	173,9	2,9	0

209

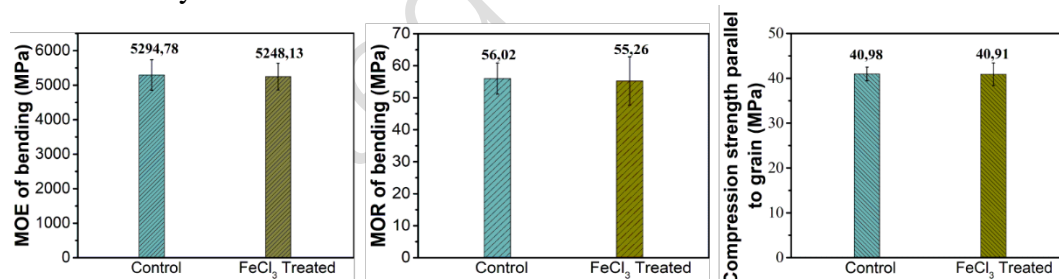


210 Figure 3 (a) shows images of control, ancient wood and FeCl<sub>3</sub> treated wood, with the latter  
 211 two exhibiting similar color while contrasting to the control. These color differences were  
 212 further quantified by the colorimeter, as shown in Figure 3 (b). As compared to the control, the  
 213 lightness  $L^*$  of FeCl<sub>3</sub> treated samples is much lower but close to that of ancient wood samples.  
 214 Similarly, the chromaticity indices  $a^*$  and  $b^*$  of the treated sample is comparable with ancient  
 215 wood samples but redder and bluer than that of the untreated samples. These results indicate  
 216 that the color of our FeCl<sub>3</sub> treated wood resembles that of ancient wood sample, which could  
 217 be further evidenced by their color difference ( $\Delta E^*$ ), as shown in Table 1.

218

### 219 Mechanical properties of FeCl<sub>3</sub> treated wood

220 The flexural and compression properties of untreated and FeCl<sub>3</sub> treated wood are shown in  
 221 Figure 4. Statistically, the inorganic salt treatment does not significantly affect the MOE, MOR  
 222 and compression strength of the samples. This is because our pretreatment time is short (Xu *et*  
 223 *al.* 2020) and NaOH solution at a lower concentration. Similar results have been reported by  
 224 Yukiko Ishikura *et al.* (2010) that the bending properties of the treated Yezo spruce samples  
 225 were not affected by NaOH solution at a concentration less than 10 %.

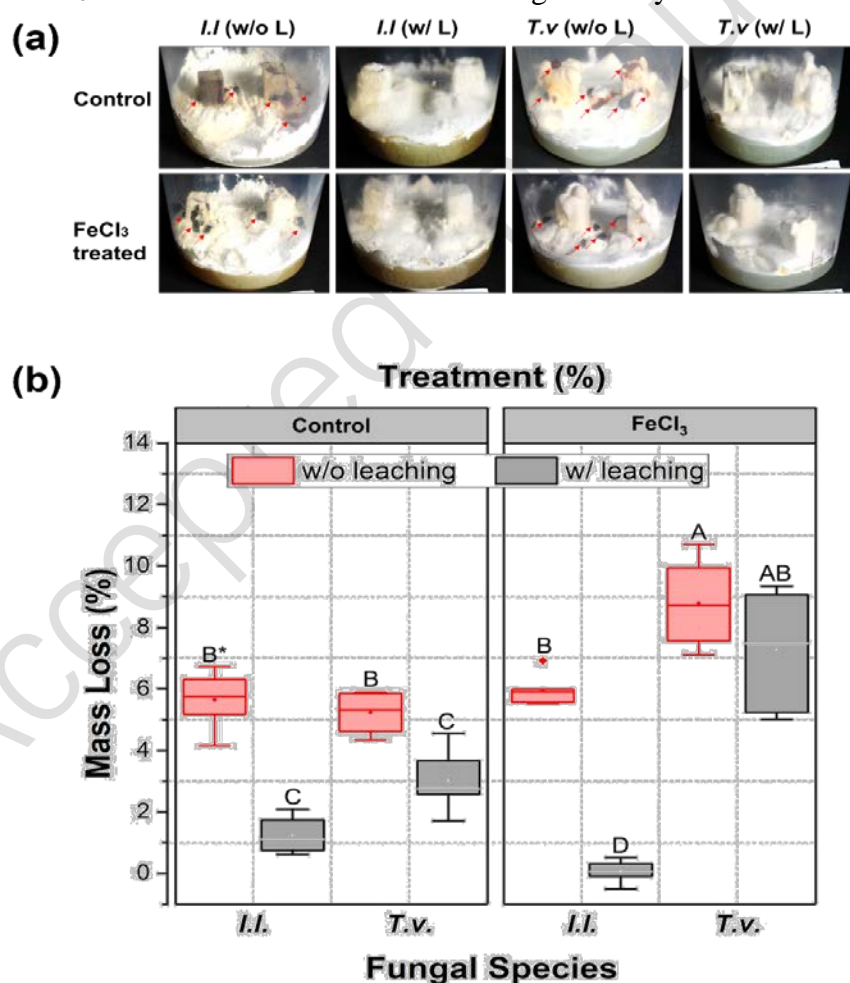


226 **Figure 4:** MOE, MOR and compression strength parallel to grain of untreated and FeCl<sub>3</sub>  
 227 treated wood.

### 228 Fungal resistance of FeCl<sub>3</sub> treated wood against white-rot fungi

229 Figure 5 shows the mass loss of control and FeCl<sub>3</sub> treated wood with and without leaching  
 230 after 8 weeks of exposure to two common white-rot fungi, *I.l.* and *T.v.*. In the control group, the  
 231 mass loss of wood samples due to white rot decay without leaching is around 4 % - 7 %, which  
 232 is significantly higher ( $p < 0,05$ ) than those of the samples with leaching (1 % - 4 %). The  
 233 relatively high mass loss of control samples without leaching could be related to the leaching  
 234 of extractives from the wood cubes during the fungi exposure period, as evident by the

235 deposition of leachate on the surface of the fungi mycelium in the culture bottles (Figure 5).  
 236 Similar results were observed for FeCl<sub>3</sub> treated samples when exposed to *I.l.*, with leached  
 237 samples recording the lowest mass loss. In comparison, there is no significant difference in  
 238 mass loss of treated samples without leaching and with leaching when exposed to *T.v.* ( $p>0,05$ ),  
 239 although both mass losses are the highest among all the tested samples ( $p>0,05$ ). These results  
 240 indicate that iron in FeCl<sub>3</sub> treated wood might have stimulated the degradation of wood by *T.v.*  
 241 (Schilling 2010), thus leading to the highest mass loss. The difference in mass loss of treated  
 242 samples exposed to the two fungi species indicates that the fungal resistance properties of FeCl<sub>3</sub>  
 243 may be fungal specific and hence varies from one fungal to the other. Overall, based on the  
 244 mass loss results, *Castanopsis sclerophylla* wood samples are resistant to the decay of both *I.l.*  
 245 and *T.v.* and FeCl<sub>3</sub> treatment on this wood does not significantly affect its durability against *I.l.*



246 **Figure 5:** a) Representative culture bottles, b) mass loss of control and FeCl<sub>3</sub> treated wood with  
 247 and without leaching after 8-week exposure to *Irpex lacteus* (*I.l.*) and *Trametes versicolor* (*T.v.*)  
 248 in an AWPA E10-16 soil block test. An arrow (↑) was used to indicate the leachates while  
 249 asterisk (\*) means that mass loss with no common letters are significantly different ( $p<0,05$ ).

---

## 250 CONCLUSIONS

251 This study proposed an effective and facile approach of archaizing wood through  
252 inorganic salts treatment. The color of FeCl<sub>3</sub> treated wood is very close to the ancient wood  
253 sample. The mechanical properties of the treated wood, including MOE, MOR and compression  
254 strength parallel to grain, are not significantly different from those in control. The FeCl<sub>3</sub> treated  
255 wood is also resistant to the decay of *I.l.* and *T.v.* and the mass losses were below 10 %,  
256 regardless of the leaching test. Therefore, this is a promising method that could be used for  
257 future historic timber buildings repair and protection.

258

## 259 AUTHORSHIP CONTRIBUTIONS

260 M. S.: Writing, original draft, Visualization Data curation; C. Z.: Visualization, Data curation;  
261 C. A.: Visualization, Data curation; Y. Y.: Supervision, Resources; L. C.: Supervision, Writing  
262 –review & editing.

263

## 264 ACKNOWLEDGMENTS

265 The authors are grateful for the financial supports from National Natural Science  
266 Foundation of China (32071684), Zhejiang Natural Science Foundation of China (No.  
267 LY16C160010), Zhejiang University Student Science and Technology Innovation Activity Plan  
268 (New Seedling talent plan subsidy project, 2022R412B043) and USDA McIntire-Stennis  
269 project under accession number NI3551. Any opinions, findings, conclusions, or  
270 recommendations expressed in the publication are those of the authors and do not necessarily  
271 reflect the view of the U.S. Department of Agriculture.

272

## 273 REFERENCES

- 274 **American Wood Protection Association. 2016a.** Standard Method for Accelerated  
275 Evaluation of Preservative Leaching. AWPA E11-16. USA.
- 276 **American Wood Protection Association. 2016b.** Laboratory method for evaluating the  
277 decay resistance of wood-based materials against pure basidiomycete cultures:  
278 soil/block test. AWPA E10-16. USA.

- 279 **Cao, J.; Wang, J.L.; Li, Y.H.; Wang, S.; Du, D.S.; Dong, M. 2015.** In-situ  
280 consolidation and restoration of wooden components in historic buildings. *J*  
281 *Northwest Univ* 30(4): 257-262. (In Chinese).  
282 [https://kns.cnki.net/kcms/detail/detail.aspx?FileName=XBLX201504043&DbName=](https://kns.cnki.net/kcms/detail/detail.aspx?FileName=XBLX201504043&DbName=CJFQ2015)  
283 [CJFQ2015](https://kns.cnki.net/kcms/detail/detail.aspx?FileName=XBLX201504043&DbName=CJFQ2015)
- 284 **Chun, Q.; Yu, M.Z.; Pan, J.W. 2013.** Research on damage characteristic and structural  
285 performance of the main hall of Baoguo temple in Ningbo. *Sci Conserv Archaeol*  
286 25(2): 45-51. (In Chinese).  
287 [https://kns.cnki.net/kcms/detail/detail.aspx?FileName=WWBF201302007&DbName](https://kns.cnki.net/kcms/detail/detail.aspx?FileName=WWBF201302007&DbName=CJFQ2013)  
288 [=CJFQ2013.](https://kns.cnki.net/kcms/detail/detail.aspx?FileName=WWBF201302007&DbName=CJFQ2013)
- 289 **Chen, Y.S.; Liu, X.Y.; Li, H.; Huang, R.F. 2005.** Issues concerning the preserving  
290 ancient timber structures. *Palace Mus J* (5): 332-343+376. (In Chinese).  
291 [https://kns.cnki.net/kcms/detail/detail.aspx?FileName=GGBW200505018&DbName](https://kns.cnki.net/kcms/detail/detail.aspx?FileName=GGBW200505018&DbName=CJFQ2005)  
292 [=CJFQ2005.](https://kns.cnki.net/kcms/detail/detail.aspx?FileName=GGBW200505018&DbName=CJFQ2005)
- 293 **Du, J.K.; Feng, X.Z.; Wang, Z.L.; Huang, Y.S.; Ramadan, E. 2002.** The methods of  
294 extracting water information from spot image. *Chin Geogr Sci* 12(1): 68-72.  
295 <https://doi.org/10.1007/s11769-002-0073-1>
- 296 **Dong, Z.Q. 2016.** Study on the mechanism of inorganic salt accelerated aging wood.  
297 M.S. Thesis, Zhejiang A&F university, Hangzhou, China. (In Chinese).
- 298 **Ding, Y.; Wan, J.; Liu, C.; Shi, X.; Xia, X.; Prakash, S.; Zhang, X. 2020.**  
299 Retrogradation properties and in vitro digestibility of wild starch from *Castanopsis*  
300 *sclerophylla*. *Food Hydrocoll* 103: 105693.  
301 <https://doi.org/10.1016/j.foodhyd.2020.105693>
- 302 **Ishikura, Y.; Abe, K.; Yano, H. 2010.** Bending properties and cell wall structure of  
303 alkali-treated wood. *Cellulose* 17(1): 47-55. [https://doi.org/10.1007/s10570-009-](https://doi.org/10.1007/s10570-009-9360-7)  
304 [9360-7](https://doi.org/10.1007/s10570-009-9360-7)
- 305 **Janin, G. 1994.** *Colorimétrie: principe de la mesure de la couleur.* Application au bois.  
306 Le bois: matériau d'ingénierie. ARBOLOR, Association pour la Recherche sur le Bois  
307 en Lorraine 10: 379-399. (In French). <https://hal.inrae.fr/hal-02843775>

- 308 **Li, J.; Zhang, F. 2007.** The characteristic research of the Hunan temple construction.  
309 *Chin Overseas Archaeol* 4: 71-73. (In Chinese).  
310 <https://kns.cnki.net/kcms/detail/detail.aspx?FileName=ZWJC200704023&DbName=CJFQ2007>.  
311
- 312 **Li, Y.J.; Lian, M.C. 2021.** Analysis on the layout of traditional residential courtyards  
313 and building structures in Guanzhong area, Shaanxi-Taking Xiaojiapo village in  
314 Lantian county as an example. In *IOP Conf Ser: Earth Environ Sci* 768(1):  
315 012141. <https://doi.org/10.1088/1755-1315/768/1/012141>
- 316 **Littell, R.C.; Henry, P.R.; Ammerman, C.B. 1998.** Statistical analysis of repeated  
317 measures data using SAS procedures. *J Anim Sci* 76(4): 1216-1231.  
318 <https://doi.org/10.2527/1998.7641216x>
- 319 **Marzi, T. 2015.** Nanostructured materials for protection and reinforcement of timber  
320 structures: A review and future challenges. *Constr Build Mater* 97: 119-130.  
321 <https://doi.org/10.1016/j.conbuildmat.2015.07.016>
- 322 **Que, Z.; Li, Z.; Zhang, X.; Yuan, Z.; Pan, B. 2017.** Traditional wooden buildings in  
323 China. Chapter 10. In *Wood in Civil Engineering*. Concu, G. (Ed.). 250 p. IntechOpen  
324 Limited, London, UK. <https://doi.org/10.5772/66145>
- 325 **Sun, Y. 2010.** Intercommunity of architectural design concepts of Chinese ancient  
326 palaces from the perspective of the Imperial Palace. *Shanxi Archi* 36(29): 18-19. (In  
327 Chinese).  
328 <https://kns.cnki.net/kcms/detail/detail.aspx?FileName=JZSX201029011&DbName=CJFQ2010>.  
329
- 330 **Shi, H.; Yong, Z.H. 2014.** Study on ancient architecture reparation technology. *J Suzhou*  
331 *Univ Sci Technol (Eng Technol)* 27(4): 68-72. (In Chinese).  
332 <https://kns.cnki.net/kcms/detail/detail.aspx?FileName=SZCJ201404015&DbName=CJFQ2014>.  
333
- 334 **Standardization Administration of the People's Republic of China. 2009a.** Method  
335 of testing in bending strength of wood. GB/T 1936.1-2009. Research Institute of  
336 Wood Industry, Chinese Academy of Forestry. China. (In Chinese).

- 337 <https://kns.cnki.net/kcms/detail/detail.aspx?FileName=SCSF00030776&DbName=S>  
338 [CSF](#)  
339 **Standardization Administration of the People's Republic of China. 2009b.** Method  
340 for determination of the modulus of elasticity in static bending of wood. GB/T  
341 1936.2-2009. Research Institute of Wood Industry, Chinese Academy of Forestry.  
342 China. (In Chinese).  
343 <https://kns.cnki.net/kcms/detail/detail.aspx?FileName=SCSF00030897&DbName=S>  
344 [CSF](#)  
345 **Standardization Administration of the People's Republic of China. 2009c.** Method  
346 of testing in compressive strength parallel to grain of wood. GB/T 1935-2009.  
347 Research Institute of Wood Industry, Chinese Academy of Forestry. China. (In  
348 Chinese).  
349 <https://kns.cnki.net/kcms/detail/detail.aspx?FileName=SCSF00030702&DbName=S>  
350 [CSF](#)  
351 **Schilling, J.S. 2010.** Effects of calcium-based materials and iron impurities on wood  
352 degradation by the brown rot fungus *Serpula lacrymans*. *Holzforschung* 64(1): 93-99.  
353 <https://doi.org/10.1515/hf.2010.009>  
354 **Triantafillou, T.C.; Deskovic, N. 1992.** Prestressed FRP sheets as external  
355 reinforcement of wood members. *J Struct Eng* 118(5): 1270-1284.  
356 [https://doi.org/10.1061/\(asce\)0733-9445\(1992\)118:5\(1270\)](https://doi.org/10.1061/(asce)0733-9445(1992)118:5(1270))  
357 **Wang, C. 2017.** Study on the mechanism of multi-inorganic salt accelerated aging wood.  
358 M.S. Thesis, Zhejiang A&F university, Hangzhou, China. (In Chinese).  
359 **Xu, E.; Wang, D.; Lin, L. 2020.** Chemical structure and mechanical properties of wood  
360 cell walls treated with acid and alkali solution. *Forests* 11(1): 87.  
361 <https://doi.org/10.3390/f11010087>  
362 **Yin, Y.R. 2019.** The integration mechanism of ancient architecture protection and  
363 modern construction. *E3S Web Conf* 136: 04036.  
364 <https://doi.org/10.1051/e3sconf/201913604036>  
365 **Yang, R.Y.; Sun, Y.F.; Zhang, X.F. 2020.** Application and progress of reinforcement

- 366 technology for Chinese ancient buildings with wood structure. *Geotech Geol Eng* 38:  
367 5695–5701. <https://doi.org/10.1007/s10706-020-01433-z>
- 368 **Yan, W.M.; Zhou, Q.; Zhang, B.; Li, Z.B. 2012.** Aseismic behavior of chinese ancient  
369 wooden structure strengthened by iron-hook. *J Beijing Univ Technol* 38(4): 502-508.  
370 (In Chinese).  
371 <https://kns.cnki.net/kcms/detail/detail.aspx?FileName=BJGD201204007&DbName=CJFQ2012>  
372 [CJFQ2012](https://kns.cnki.net/kcms/detail/detail.aspx?FileName=BJGD201204007&DbName=CJFQ2012)
- 373 **Yang, J. 2019.** From materials: enlightenment of wood selection and application in  
374 ancient Chinese timber buildings. *Res Archit Hist Theory* 4: 101-106. (In Chinese).  
375 <https://kns.cnki.net/kcms/detail/detail.aspx?FileName=JZSS201904016&DbName=CJFQ2019>  
376 [JFQ2019](https://kns.cnki.net/kcms/detail/detail.aspx?FileName=JZSS201904016&DbName=CJFQ2019)
- 377 **Zhang, H.M.; Yang, S.G.; Zhang, Y.J.; Lu, X.; Li, Y.F.; Tao, B. 2013.** Characteristics  
378 of ancient building lightning disasters. *Meteorol Sci Technol* 41(4): 758-763. (In  
379 Chinese).  
380 <https://kns.cnki.net/kcms/detail/detail.aspx?FileName=QXKJ201304027&DbName=CJFQ2013>.  
381 [CJFQ2013](https://kns.cnki.net/kcms/detail/detail.aspx?FileName=QXKJ201304027&DbName=CJFQ2013).
- 382 **Zhao, X.B.; Zhang, F.L.; Xue, J.Y.; Ma, L.L. 2019.** Shaking table tests on seismic  
383 behavior of ancient timber structure reinforced with CFRP sheet. *Eng Struct* 197:  
384 109405. <https://doi.org/10.1016/j.engstruct.2019.109405>
- 385 **Zhou, K.; Li, A.; Xie, L.L.; Wang, C.C.; Wang, P.; Wang, X.F. 2020.** Mechanism and  
386 effect of alkoxysilanes on the restoration of decayed wood used in historic buildings.  
387 *J Cult Herit* 43: 64-72. <https://doi.org/10.1016/j.culher.2019.11.012>
- 388 **Zhang, T.; Yang, P.; Chen, M.Z.; Yang, K.; Cao, Y.Z.; Li, X.H.; Tang, M.; Chen,  
389 W.M.; Zhou, X.Y. 2019.** Constructing a novel electroluminescent device with high-  
390 temperature and high-humidity resistance based on a flexible transparent wood film.  
391 *ACS Appl Mater Interfaces* 11(39): 36010-36019.  
392 <https://doi.org/10.1021/acsami.9b09331>.

393